Protein-based molecular contrast optical coherence tomography with phytochrome as the contrast agent

Changhuei Yang and Michael A. Choma

Department of Biomedical Engineering, 136 Hudson Hall, Duke University, Durham, North Carolina 27708

Laura E. Lamb and John D. Simon

Department of Chemistry, 101 Gross Chemistry Laboratory, Duke University, Durham, North Carolina 27708

Joseph A. Izatt

Department of Biomedical Engineering, 136 Hudson Hall, Duke University, Durham, North Carolina 27708

Received January 2, 2004

We report the use of phytochrome A (phyA), a plant protein that can reversibly switch between two states with different absorption maxima (at 660 and 730 nm), as a contrast agent for molecular contrast optical coherence tomography (MCOCT). Our MCOCT scheme builds up a difference image revealing the distribution of phyA within a target sample from pairs of consecutive OCT A-scans acquired at a probe wavelength of 750 nm, both with and without additional illumination of the target sample with 660-nm light. We demonstrate molecular imaging with this new MCOCT modality in a target sample containing a mixture of 0.2% Intralipid and 83 μM of phyA.

OCIS codes: 110.4500, 170.3880, 300.6390, 350.5130.

Optical coherence tomography[1,2] (OCT) is an excellent optical bioimaging modality for extracting highly resolved structural information on biological samples to a depth of a few millimeters. Although various functional OCT methods have extended the range of information that can be extracted to include flow properties[3] (Doppler) and tissue organization (birefringence),[4] it is only recently that the capability to detect specific contrast agents (chemical[5] and otherwise[6]) with OCT has seen significant research development. This extension of OCT technology, which we classify as molecular contrast optical coherence tomography (MCOCT), combines the major advantages of fluorescence microscopy[7] and OCT, i.e., the contrast agent specificity of the former and the higher spatial resolution and depth penetration of the latter. The rapid and widespread adaptation of fluorescence microscopy techniques based on green fluorescence protein[8] in biology research points to the usefulness of imaging modalities based on contrast agents, especially if the contrast agent in question is endogenous and (or) amenable to transfection as a label for targeted gene expression.

In this Letter we present what is to our knowledge the first MCOCT implementation that is capable of profiling the distribution of a specific protein within a target sample. The protein, phytochrome A (phyA),[9] is endogenous to all plants and serves as part of the photoperiodic mechanism. This protein can reversibly switch between two states with different absorption maxima on illumination with light of suitable wavelengths. We report on the conditions for state switching, quantify the relative absorption change, and demonstrate a feasible MCOCT scheme that exploits the absorption change to profile the protein's distribution within a target sample. Finally, we show an experimental implementation of the method and demonstrate its capability in localizing the protein in a tissue-simulating scattering phantom.

To understand our MCOCT scheme, a detailed examination of phyA's dynamics is required. We acquired phyA samples (Kumho Laboratory) purified from dark-grown oats. The dynamics and properties of the two states of phyA (Pfr and Pr states) are summarized in Fig. 1. The molecules can be made to transit from one state to the other by illumination with light of a wavelength that matches the absorption maximum of the initial state. The transit time scale for the state changes is strongly dependent on the light intensities employed. The characteristic ($1/e$) times of the order of ~150 ms in both transit directions were observed with an illumination intensity level of ~200 mW/cm^2. The Pfr state is the more stable state; the molecules will revert to this state within several seconds in the absence of any significant illumination.

The imaging strategy that we adopted for phyA is based on acquiring OCT scans at 750 nm while

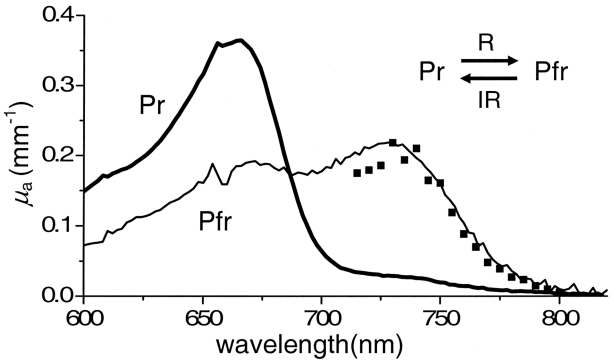

Fig. 1. Absorption spectra of 83-μM phyA in its native Pr state and in its Pfr state following strong illumination (>1 W/cm^2 of 750-nm light) at 730 nm. (Data were acquired by transmission measurements in a HP8452A spectrophotometer.) The squares represent the observed absorption coefficient change at different potential MCOCT probe wavelengths under illumination by the pump light (intensity ~200 mW/cm^2) at wavelength 660 nm.

0146-9592/04/121396-03$15.00/0

switching the molecules between their two states. To this end, we kept a 750-nm OCT probe beam on the sample during the entire imaging process; in the absence of other illumination, phyA would be in its Pr state. The wavelength was chosen as a compromise between the Pfr absorption maximum wavelength and the optimal OCT wavelength. The image acquisition process involved the following steps: (A) the 660-nm illumination was switched on, (B) after a pause of 500 ms to allow time for phyA to transit into its Pfr state, an averaged Pfr A-scan was acquired, (C) the 660-nm light was turned off, (D) after a pause of 500 ms to allow phyA to transit into its Pr state, an averaged Pr A-scan was acquired, and (E) the sample was displaced laterally and the process was repeated.

To effectively switch a significant proportion of phyA from the Pr state to the Pfr state in step (B), the intensity ratio of 660-nm pump light to 750-nm probe light must be sufficiently large. To our knowledge this ratio has not been reported in the literature. We determine this ratio in a separate transmission-based experiment in which the pump and probe beams copropagated through a cuvette of phyA. We varied the intensity of the 750-nm probe light while modulating the pump beam and inferred the population shift from the measured transmission at the probe wavelength. Mathematically, the ratio of 660-nm pump light intensity ($I_{660\mathrm{nm}}$) to 750-nm probe light intensity ($I_{750\mathrm{nm}}$) required for a state change in the protein is governed by the rate equation

$$\frac{\mathrm{d}n_{\mathrm{Pfr}}}{\mathrm{d}t} = \frac{(n_0 - n_{\mathrm{Pfr}})}{\tau_{\mathrm{Pr}}} - \frac{\sigma_{\mathrm{Pfr},750\mathrm{nm}}\varepsilon_{\mathrm{IR}}}{h\nu_{750\mathrm{nm}}} I_{750\mathrm{nm}} n_{\mathrm{Pfr}} + \frac{\sigma_{\mathrm{Pr},660\mathrm{nm}}\varepsilon_R}{h\nu_{660\mathrm{nm}}} I_{660\mathrm{nm}}(n_0 - n_{\mathrm{Pfr}}), \quad (1)$$

where n_0 is the total phyA concentration, n_{Pfr} is the concentration of phyA in the Pfr state, $h\nu$ is the photon energy at the wavelength indicated by the subscript, $\sigma_{\mathrm{Pfr},750\mathrm{nm}}$ ($\sigma_{\mathrm{Pr},660\mathrm{nm}}$) is the absorption cross section of the Pfr (Pr) state at 750 nm (660 nm), τ_{Pr} is the natural decay time of the Pr state to the Pfr state (this term is very weak in the presence of pump light and shall henceforth be ignored), and ε_R and $\varepsilon_{\mathrm{IR}}$ are the quantum efficiencies of the transition from Pr to Pfr and vice versa, respectively. Under steady-state conditions, we obtain

$$\frac{n_{\mathrm{Pfr}}}{n_0} \approx 1/1 + \frac{\nu_{660\mathrm{nm}}\varepsilon_{\mathrm{IR}}\sigma_{\mathrm{Pfr},750\mathrm{nm}}}{\nu_{750\mathrm{nm}}\varepsilon_R\sigma_{\mathrm{Pr},660\mathrm{nm}}} \frac{I_{750\mathrm{nm}}}{I_{660\mathrm{nm}}} = \frac{1}{1 + a(I_{750\mathrm{nm}}/I_{660\mathrm{nm}})}, \quad (2)$$

where a represents a characteristic rate factor for the transition dynamic. For phyA we determined this factor to be (1.82 ± 0.18) from a fit of approximation (2) to the experimental data shown in Fig. 2. This characterization informs us that a light intensity ratio of ~ 4 should cause a significant population shift ($\sim 75\%$) in the molecules' states.

The phytochrome MCOCT experimental setup is depicted in Fig. 3. A tunable femtosecond Ti:sapphire laser (Spectra-Physics Tsunami) with a FWHM linewidth of 11 nm (resulting in a calculated coherence length of 25 μm) served as the OCT probe light source and was coupled into the setup. Part of the source light comprising the reference arm of the interferometer with power P_{Ro} was retroreflected and recoupled back into the interferometer. The scanning retroreflector created a Doppler frequency upshift of 41 kHz on the reflected reference beam. The remainder of the source light with power P_{So} was combined with 660-nm light from a Power Technology PPM20/6393 laser diode in a custom dichroic combiner (OZ Optics). The combined beam was then focused (Newport M-20× objective) onto a target sample, and the backscattered light (signal) was recoupled back into the interferometer. The FWHM of the focal spot and the depth of focus on the sample were calculated to be 6.9 and 124 μm, respectively. The typical 750- and 660-nm powers that were incident upon the sample during image data acquisition were 104 and 433 μW, respectively, to satisfy the intensity ratio requirement. The interfering signal and reference light were detected using a New Focus Model 2007 autobalanced detector. The 660-nm illumination was modulated by an OZ Optics transistor–transistor logic gated optical switch. The system acquired 2-mm optical path length A-scans at a rate of approximately 5 Hz.

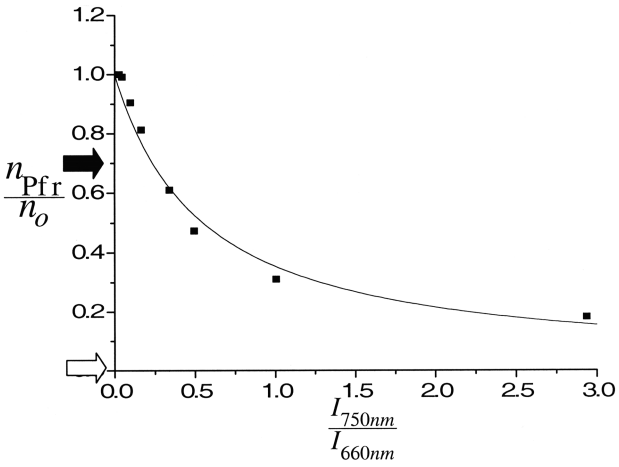

Fig. 2. Plot of the observed fractional phyA population undergoing state change versus the ratio of 750-nm probe light to modulated 660-nm pump light intensity used. The solid curve is the best fit of the data to approximation (2). The filled (open) arrow shows the expected population ratio of phyA in the Pfr state for step (B) [step (D)] of the imaging sequence under the chosen experimental parameters.

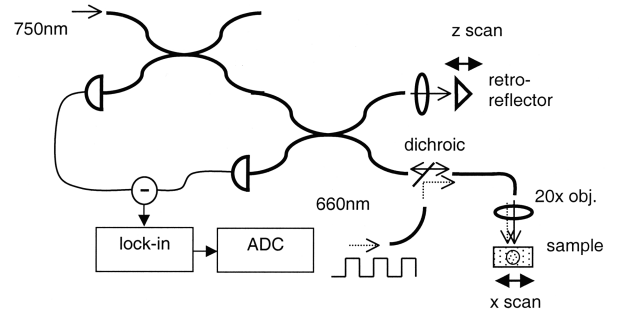

Fig. 3. Schematic of the MCOCT experimental setup. ADC, analog-to-digital converter.

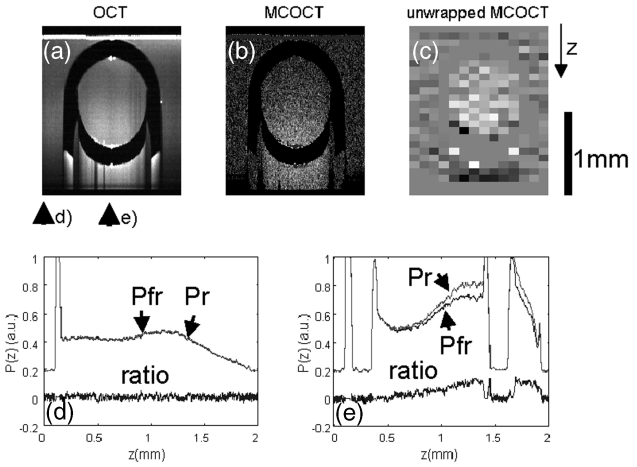

Fig. 4. (a) 750-nm OCT B-scan with phyA in the Pr state (1.5 mm wide × 2 mm deep); the OCT B-scan with phyA in the Pfr state appears to be similar (not shown). (b) MCOCT differential scan derived based on the operations described in Eq. (4). (c) Unwrapped MCOCT scan derived based on the operations described in Eq. (5). (d) A-scans with phyA in the Pr and Pfr states extracted from the locations indicated by the arrows in (a). (e) A-scans with phyA in the Pr and Pfr states extracted from the locations indicated in (a).

Figure 4(a) shows a 300 × 4000 pixel B-scan (lateral step 5 μm) created by compiling averaged A-scans (300-scan average) acquired in the above-mentioned imaging sequence. The sample comprised a 1-mm-thick capillary tube containing 83 μM of phyA in 0.2% Intralipid inserted into a 2-mm cuvette filled with 0.2% Intralipid. Figures 4(d) and 4(e) show averaged Pfr and Pr A-scans along different positions of the sample. Not surprisingly the Pfr and Pr A-scans show a difference only for the pair that was acquired across the capillary containing phyA. The increasing difference at greater depth is due to the cumulative effect of absorption on the OCT signal. More explicitly, the OCT signal, $P(z)$, from a given depth z in the sample is given by

$$P(z) = 2\sqrt{P_{\mathrm{So}}P_{\mathrm{Ro}}}\sqrt{R(z)}\exp\left[-\int_0^z \mu_a(z') + \mu_a(z')\mathrm{d}z'\right], \tag{3}$$

where $R(z)$ is the depth-dependent collected backscattered light from the sample (which includes effects due to focal parameters) and $\mu_a(z)$ and $\mu_s(z)$ are the extinction and scattering coefficients at depth z, respectively. Between Pfr and Pr A-scans, $\mu_a(z)$ is changed significantly, and its presence in the integration term of Eq. (3) leads to a cumulative increase in the signal difference. We can use this analysis to generate an image of $\mu_a(z)$ by processing the Pfr, $P_{\mathrm{Pr}}(z)$ and Pr, $P_{\mathrm{Pfr}}(z)$ scans:

$$\ln\left[\frac{P_{\mathrm{Pr}}(z)}{P_{\mathrm{Pfr}}(z)}\right] = \int_0^z \mu_{a,\mathrm{Pfr}}(z') - \mu_{a,\mathrm{Pr}}(z')\mathrm{d}z' = \int_0^z \Delta\mu_a(z')\mathrm{d}z'. \tag{4}$$

Figure 4(b) shows the result of such processing. This image clearly shows the distribution of phyA in the sample as being within the capillary tube. Figures 4(d) and 4(e) show the processed A-scans along different positions of the sample. The observed $\Delta\mu_a$ of (0.14 ± 0.2) mm^{-1} is in good agreement with the predicted value of 0.12 mm^{-1} based on the concentration of phyA.

The processed scans can be further processed and unwrapped to eliminate the integrative effect. Mathematically, the processing is

$$\ln\left[\frac{P_{\mathrm{Pr}}(z+\Delta z)}{P_{\mathrm{Pfr}}(z+\Delta z)}\right] - \ln\left[\frac{P_{\mathrm{Pr}}(z)}{P_{\mathrm{Pfr}}(z)}\right] = \int_z^{z+\Delta z} \Delta\mu_a(z')\mathrm{d}z' \approx \Delta\mu_a(z)\Delta z\,. \tag{5}$$

Because of the derivative nature of this processing, it is highly susceptible to noise. Figure 4(c) shows the result when $\Delta z = 80$ μm was used and spatial averaging over 20 × 160 pixels was done. The heightened signal within the capillary indicates phyA's presence.

In a separate experiment to detect any photoinduced damage on phyA, we subjected the phytochrome to 1000 cycles of Pr → Pfr → Pr change. The amount of contrast change did not degrade to any observable extent throughout the entire experiment.

In conclusion, we have demonstrated what is believed to be the first implementation of molecular contrast optical coherence tomography using a protein as a probe molecule. The extension of MCOCT to protein molecular imaging is significant, as it opens the possibility of MCOCT imaging of genetic expression of molecular probes in the same manner that fluorescent proteins are employed in fluorescence-based molecular imaging. PhyA could thus potentially fulfill the role of an endogenously expressed contrast agent for MCOCT.

This research was supported by National Institutes of Health grant EB000243. C. Yang's e-mail address is chyang@caltech.edu.

References

1. A. F. Fercher, J. Biomed. Opt. **1,** 157 (1996).
2. J. M. Schmitt, IEEE J. Sel. Top. Quantum Electron. **5,** 1205 (1999).
3. J. A. Izatt, M. D. Kulkarni, S. Yazdanfar, J. K. Barton, and A. J. Welch, Opt. Lett. **22,** 4139 (1997).
4. J. F. deBoer, T. E. Milner, M. J. C. vanGemert, and J. S. Nelson, Opt. Lett. **22,** 934 (1997).
5. K. D. Rao, M. A. Choma, S. Yazdanfar, A. M. Rollins, and J. A. Izatt, Opt. Lett. **28,** 340 (2003).
6. T. M. Lee, A. L. Oldenburg, S. Sitafalwalla, D. L. Marks, W. Luo, F. J. J. Toublan, K. S. Suslick, and S. A. Boppart, Opt. Lett. **28,** 1546 (2003).
7. W. Denk, J. H. Strickler, and W. W. Webb, Science **248,** 73 (1990).
8. R. H. Kohler, W. R. Zipfel, W. W. Webb, and M. R. Hanson, Plant J. **11,** 613 (1997).
9. C. Fankhauser, J. Biol. Chem. **276,** 11453 (2001).